Radboud University Nijmegen

Faculty of Science

Mass Clumping Effects on a Cosmological Model

Thesis BSc Physics and Astronomy

Supervisor:
prof. dr. Wim Beenakker
David Venhoek

Author:
Wouter Morren

Second reader:
prof. Andrew Levan

Institute for Mathematics, Astrophysics and Particle Physics
High-Energy Physics

July 2021

Contents

1 Introduction

For quite some years now, physicists all over the world have been trying to understand the discrepancy between two different measured values of the Hubble parameter. One value is determined from measurements on the CMB from the early universe and the other from standard candles in the late universe [1]. Early-time measurements by the Planck collaboration give a value for the Hubble parameter of $H_0 = 67.36 \pm 0.54$ km s^{-1} Mpc^{-1} [2]. Multiple late-time measurements combined resulted in a value of $H_0 = 73.3 \pm 0.8$ km s^{-1} Mpc^{-1} [3]. Both values lie outside each other's error margin and this gives rise to the need for an explanation to account for this discrepancy.

Currently, most cosmological models are based on the quite successful Friedmannian model, which assumes that our universe is homogeneously distributed at all scales. This is confirmed to be true on large scales, but this does not necessarily mean that the inhomogeneity on small scales can be neglected. This homogeneity assumption can be translated to a universe having a constant spatial curvature at any given time. This property has then been used to derive the Friedmann-Robertson-Walker (FRW) metric, which was thereafter plugged into the Einstein Field Equations (EFE). Moreover, in the Friedmannian model, it is assumed that the matter and energy in our universe can be modelled as a perfect fluid. The corresponding stress-energy tensor in the EFE in that case takes a very simple form. Those two assumptions together simplify the EFE, from which an equation for the Hubble parameter can be derived.

Since the Friedmannian model causes a tension between the two obtained Hubble parameters, this model is perhaps not entirely correct. On one hand, maybe one should not neglect inhomogeneity on small scales. On the other hand, perhaps the matter and energy in the universe can in the end not be modelled as a perfect fluid, causing the stress-energy tensor to take a more complicated form. Consequently, if such is the case, this may explain the discrepancy between the two different Hubble parameters.

In this thesis, we therefore test a universe consisting of mass clumps and, consequently, we omit the aforementioned two assumptions of the Friedmannian model, at least on small scales. Moreover, we would like to determine the effects of this mass clumping on the properties of the universe. Heinesen and Buchert, in 2020 [4], proposed a solution to the discrepancy in the two values of the Hubble parameter

by adding an extra term to the stress-energy tensor, which they claim to arise from structure formation. Hence it is interesting to more specifically investigate how mass clumping may result in this solution.

Unfortunately it is impossible to describe the entire universe, hence simplifications have to be made. One possible model is that of a static universe being made up of numerous mass clumps. These mass clumps can be simplified to spheres, all having the same radius R and constant density ρ. Since our universe is expanding at an accelerating pace, a non-zero cosmological constant will be used throughout all calculations. We do so because we do not necessarily expect or aim to obtain a cosmological model that provides an explanation for dark energy as well. The metric for such a spherical mass clump is derived in section 2.

To be able to use these mass clumps to describe a universe that is homogeneous at large scales, we placed the spheres on an infinitely large grid. Since it is impossible to derive the exact metric of the entire universe, consisting of those periodically placed mass clumps, we have made some more simplifications and applied tricks to create a metric that approximately resembles our toy universe. This will be done in section 3.

Due to the simplifications, our modelled universe can be described entirely by only a few different discrete regions and their corresponding metrics. These separate metrics will then be used to derive the time component of the stress-energy tensor per region. Consequently, the time component of the stress-energy tensor of the entire modelled universe will not simply be a certain energy density anymore, as in a perfect fluid. However, using the requirement that the universe at large is in fact homogeneous, we can still calculate the average energy density of our toy universe, which will be done in section 4.

This resulting average density can then be compared to the energy density that the Friedmannian model would give us, taking into account the properties of our toy universe. Any difference in the two obtained values may indicate that extra energy density contributions arise when taking mass clumping into account.

2 Metric of a single mass clump

2.1 Setting up the EFE

In this chapter, we will explain step by step, how we obtain the metric of a sphere with a uniform density and a non-zero cosmological constant. We will do so by demanding that at the edge of the sphere, this metric should coincide with the Schwarzschild metric from outside the sphere. For the derivation of this metric, we use the same technique as Carroll [5], only we have started the derivation using the EFE with a non-zero cosmological constant Λ:

$$R_{\mu\nu} - \frac{1}{2}Rg_{\mu\nu} + \Lambda g_{\mu\nu} = 8\pi G T_{\mu\nu}. \tag{1}$$

Note that we use the convention in which we do not put the Λ term into our stress-energy tensor. Moreover, for the time being, we use natural units, i.e. $c = 1$.

We are currently considering a static, spherically symmetric metric, hence we can start our derivation using the following general metric:

$$ds^2 = -e^{2\bar{\alpha}(\bar{r})}dt^2 + e^{2\bar{\beta}(\bar{r})}d\bar{r}^2 + e^{2\bar{\gamma}(\bar{r})}\bar{r}^2 d\Omega^2, \text{ where } d\Omega^2 = d\theta^2 + sin^2\theta d\phi^2. \tag{2}$$

It is important to note that using this definition of the metric, we will from now on use the mostly plus convention for any metric. As you can see, the functions inside the exponentials are only dependent on the radial coordinate, such that the metric is indeed spherically symmetric. In this general metric we used $\bar{r}$ as the radial coordinate. We can now make a change in the radial coordinate to simplify the metric in order to make the following calculations easier. Consequently, the meaning of the new radial coordinate r is hard to visualise, but we can interpret the result in the end nonetheless. So let us take $r = \bar{r}e^{\bar{\gamma}(\bar{r})}$ and rewrite the metric, such that:

$$ds^2 = -e^{2\alpha(r)}dt^2 + e^{2\beta(r)}dr^2 + r^2 d\Omega^2. \tag{3}$$

Now $\alpha(r)$ and $\beta(r)$ are different functions than $\bar{\alpha}(\bar{r})$ and $\bar{\beta}(\bar{r})$. Using this general metric, the non-zero Christoffel symbols, as given by Carroll, are:

$$\begin{aligned}
&\Gamma^t_{tr} = \partial_r\alpha && \Gamma^r_{tt} = e^{2(\alpha-\beta)}\partial_r\alpha && \Gamma^r_{rr} = \partial_r\beta \\
&\Gamma^\theta_{r\theta} = \frac{1}{r} && \Gamma^r_{\theta\theta} = -re^{-2\beta} && \Gamma^\phi_{r\phi} = \frac{1}{r} \\
&\Gamma^r_{\phi\phi} = -re^{-2\beta}\sin^2\theta && \Gamma^\theta_{\phi\phi} = -\sin\theta\cos\theta && \Gamma^\phi_{\theta\phi} = \frac{\cos\theta}{\sin\theta}
\end{aligned} \tag{4}$$

Next we will use the following definition of the Ricci tensor:

$$R_{\mu\nu} = R^{\lambda}_{\mu\lambda\nu} = \frac{\partial\Gamma^{\lambda}_{\mu\nu}}{\partial x^{\lambda}} - \frac{\partial\Gamma^{\lambda}_{\mu\lambda}}{\partial x^{\nu}} + \Gamma^{\sigma}_{\mu\nu}\Gamma^{\lambda}_{\sigma\lambda} - \Gamma^{\sigma}_{\mu\lambda}\Gamma^{\lambda}_{\sigma\nu} \tag{5}$$

From this, the components of the Ricci tensor and then the Ricci scalar can be calculated:

$$R_{tt} = e^{2(\alpha-\beta)}\left[\partial_r^2\alpha + (\partial_r\alpha)^2 - \partial_r\alpha\partial_r\beta + \frac{2}{r}\partial_r\alpha\right] \tag{6}$$

$$R_{rr} = -\left[\partial_r^2\alpha + (\partial_r\alpha)^2 - \partial_r\alpha\partial_r\beta - \frac{2}{r}\partial_r\beta\right] \tag{7}$$

$$R_{\theta\theta} = e^{-2\beta}\left[r(\partial_r\beta - \partial_r\alpha) - 1\right] + 1 \tag{8}$$

$$R_{\phi\phi} = R_{\theta\theta}\sin^2\theta \tag{9}$$

$$R = -2e^{-2\beta}\left[\partial_r^2\alpha + (\partial_r\alpha)^2 - \partial_r\alpha\partial_r\beta + \frac{2}{r}(\partial_r\alpha - \partial_r\beta) + \frac{1}{r^2}(1 - e^{2\beta})\right] \tag{10}$$

Having all the components of the l.h.s. of the EFE (equation 1) at this point, let us have a look at the components of the r.h.s., i.e. the stress-energy tensor. Assuming the mass sphere to be a static perfect fluid we can take the four-velocity of the sphere to be pointing in the time direction only. Normalising the four-velocity $U^{\mu}U_{\mu} = -1$, we get the velocity $U_{\mu} = \frac{dx_{\mu}}{d\tau} = (e^{\alpha}, 0, 0, 0)$ and hence

$$T_{\mu\nu} = (\rho + p)U_{\mu}U_{\nu} + pg_{\mu\nu} = \begin{pmatrix} e^{2\alpha}\rho & & & \\ & e^{2\beta}p & & \\ & & r^2p & \\ & & & r^2\sin^2(\theta)p \end{pmatrix}. \tag{11}$$

Finally, we can get the tt component of the EFE,

$$e^{-2\beta}[2r\partial_r\beta - 1] + 1 - r^2\Lambda = 8\pi G r^2\rho, \tag{12}$$

and the rr component,

$$e^{-2\beta}[2r\partial_r\alpha + 1] - 1 + r^2\Lambda = 8\pi G r^2 p. \tag{13}$$

We do not need the other two components in our calculations.

2.2 Matching Schwarzschild: g_{rr}

Now that we have a useful set of equations, we will in this section impose some constraints on the metric inside the sphere in order to obtain g_{rr}. At the edge of the sphere we require all of the components of this metric to coincide with the Schwarzschild metric from outside the sphere. Hence we need the Schwarzschild metric for $\Lambda \neq 0$ [6], which is

$$ds^2 = -\left[1 - \frac{2GM}{r} - \frac{r^2\Lambda}{3}\right]dt^2 + \left[1 - \frac{2GM}{r} - \frac{r^2\Lambda}{3}\right]^{-1} dr^2 + r^2 d\Omega^2. \tag{14}$$

In order for our metric to coincide with the Schwarzschild metric at $r = R$, it is convenient to write one of the components of our metric in a similar way. We can for instance write

$$g_{rr} = e^{2\beta} = \left[1 - \frac{2Gm(r)}{r} - \frac{r^2\Lambda}{3}\right]^{-1}, \tag{15}$$

such that

$$m(r) = -\frac{r}{2G}\left(e^{-2\beta} - 1 + \frac{r^2\Lambda}{3}\right). \tag{16}$$

We can interpret $m(r)$ as the mass of the sphere lying within a radius r. Hence at $r = R$ this expression should be equal to the total mass inside the sphere, which is $m(R) = M$. This is not equal to the real mass of the sphere as we are working in a different coordinate system, but this will be accounted for in section 4.3. For more insights into the meaning of M, please have a look at appendix A. For now let us continue the derivation. Taking the derivative of $m(r)$ with respect to r gives us:

$$\frac{dm}{dr} = \frac{1}{2G}(e^{-2\beta}[2r\partial_r\beta - 1] + 1 - r^2\Lambda) = 4\pi r^2\rho, \tag{17}$$

where the tt component of the EFE has been substituted to obtain this well known result. Consequently, $m(r) = \frac{4}{3}\pi r^3\rho$ and hence we find that at the edge of the sphere $m(R) = \frac{4}{3}\pi R^3\rho = M$, such that $m(r) = Mr^3/R^3$. Therewith, we can write the radial component of the metric more conveniently as:

$$g_{rr} = e^{2\beta} = [1 - kr^2]^{-1}, \quad \text{where} \quad k = \frac{2GM}{R^3} + \frac{\Lambda}{3}. \tag{18}$$

2.3 Solving by energy conservation: g_{tt}

The next step is to determine the time component of the metric inside the sphere. Remember that we will need to determine the function $\alpha(r)$ in that case, since

$g_{tt} = -e^{2\alpha(r)}$. Substituting the radial component of the metric g_{rr}, i.e. equation 18, into the rr component of the EFE, i.e. equation 13, one can get an expression for the partial derivative of α:

$$\partial_r \alpha = \frac{4\pi G[p(r) + \frac{\rho}{3}] - \frac{\Lambda}{3}}{1 - kr^2} r \tag{19}$$

To be able to integrate this expression, we will need to know the equation for $p(r)$. Hence, for the next step we are particularly interested in the r component of the energy conservation equations, being

$$\nabla_\mu T^{\mu r} = 0, \tag{20}$$

in which μ is summed over. For this we need the inverse stress-energy tensor:

$$T^{\mu\nu} = g^{\mu\gamma} g^{\nu\delta} T_{\gamma\delta} = \begin{pmatrix} e^{-2\alpha}\rho & & & \\ & e^{-2\beta}p & & \\ & & r^{-2}p & \\ & & & r^{-2}\sin^{-2}(\theta)p \end{pmatrix} \tag{21}$$

Then, using the definition of the tensor derivative

$$\nabla_\sigma T^{\mu\nu} = \partial_\sigma T^{\mu\nu} + \Gamma^\mu_{\sigma\lambda} T^{\lambda\nu} + \Gamma^\nu_{\sigma\lambda} T^{\mu\lambda}, \tag{22}$$

and setting $\sigma = \mu$ and $\nu = r$, we can obtain the r component of the energy conservation equation. Only the terms for which μ equals t or r are non-zero, giving us

$$\nabla_\mu T^{\mu r} = e^{-2\beta}[\partial_r p + \partial_r \alpha(p + \rho)] = 0, \tag{23}$$

such that

$$\partial_r p = -(p + \rho)\partial_r \alpha. \tag{24}$$

This differential equation can be solved by substituting the partial derivative of α from equation 19 into equation 24. Then by separating the variables r and p we obtain the equation

$$-3 \int \frac{dp}{(p + \rho)(4\pi G(3p + \rho) - \Lambda)} = \int \frac{r dr}{1 - kr^2} \tag{25}$$

At the edge of the sphere and beyond, the density of the sphere becomes zero, and so does the pressure. Hence we demand that $p = 0$ at $r = R$ for determining the integration constant, giving us the pressure as a function of radius:

$$p(r) = \rho \frac{\sqrt{1 - kR^2} - \sqrt{1 - kr^2}}{q\sqrt{1 - kR^2} + \sqrt{1 - kr^2}}, \text{ where } q = \frac{3\rho}{2\rho_{vac} - \rho}. \tag{26}$$

Here we have used that $\Lambda = 8\pi G\rho_{vac}$, with ρ_{vac} being the vacuum mass density, to express this equation more elegantly. However, in the final expression of the metric we will be writing the dark energy terms back in terms of Λ as this is a more familiar quantity than ρ_{vac}. When using that $\Lambda = 8\pi G\rho_{vac}$ and $M = \frac{4}{3}\pi R^3\rho$, we can write $k = \frac{8}{3}\pi G(\rho + \rho_{vac})$. Now the above equation for the pressure can be inserted into equation 19 describing $\partial_r\alpha$. Then, using the other form of k, this equation can be rewritten to obtain:

$$\alpha = \int \frac{-krdr}{\sqrt{1-kr^2}(q\sqrt{1-kR^2}+\sqrt{1-kr^2})} = \ln\left(q\sqrt{1-kR^2}+\sqrt{1-kr^2}\right) + C \quad (27)$$

Since we have two boundary conditions to take into account, we define the integration constant as $C = \ln(C_1C_2)$, where C_1 and C_2 are two yet to be determined constants. Consequently, we can obtain the following expression for g_{tt}:

$$g_{tt} = -e^{2\alpha} = -\left[\left(q\sqrt{1-kR^2}+\sqrt{1-kr^2}\right)C_1C_2\right]^2. \quad (28)$$

The two boundary conditions can now be used for determining these constants. First of all, we require that for $\Lambda = 0$ (i.e. $\rho_{vac} = 0$), the time component of our metric $g_{tt} = -e^{2\alpha}$ should reduce to the time component of the metric of a uniform sphere, derived by Carroll [5]:

$$g_{tt}^{\Lambda=0} = -\left[\frac{3}{2}\sqrt{1-\frac{2GM}{R}} - \frac{1}{2}\sqrt{1-\frac{2GMr^2}{R^3}}\right]^2 = -\left[\frac{3}{2}\sqrt{1-k_0R^2} - \frac{1}{2}\sqrt{1-k_0r^2}\right]^2 \quad (29)$$

Here k_0 is simply $k(\Lambda = 0) = 2GM/R^3$. For $\rho_{vac} = 0$, as a first step, we require for instance that C_2 must equal 1. Moreover, for $\rho_{vac} = 0$ we get $q = -3$ and hence we can observe that C_1 should equal $-\frac{1}{2}$ in order to obtain the fractions $\frac{3}{2}$ and $-\frac{1}{2}$ in equation 29.

Secondly, at $r = R$ the time component of our metric $g_{tt} = -e^{2\alpha}$ should reduce to the time component of the Schwarzschild metric from equation 14, such that our metric can smoothly flow into the Schwarzschild metric at the edge of the sphere. Remember that for $r = R$ the time component of the Schwarzschild metric reads $g_{tt}^S = -(1-kR^2)$. Hence, knowing that $C_1 = -\frac{1}{2}$ it follows that $C_2 = -2(q+1)^{-1}$, which is indeed equal to 1 for $\Lambda = 0$. Consequently, $C_1C_2 = (q+1)^{-1}$ and therewith, when writing out the definition of q, we get

$$g_{tt} = -\left[\frac{1}{2(\rho+\rho_{vac})}(3\rho\sqrt{1-kR^2} + (2\rho_{vac}-\rho)\sqrt{1-kr^2})\right]^2 \quad (30)$$

Again using that $\Lambda = 8\pi G\rho_{vac}$ and $k = \frac{8}{3}\pi G(\rho + \rho_{vac})$, g_{tt} can be rewritten, giving us the final metric for a sphere with uniform density and $\Lambda \neq 0$:

$$\begin{aligned} ds^2 &= -\frac{1}{k^2}\Big[l\sqrt{1-kR^2} - \big(l-k\big)\sqrt{1-kr^2}\Big]^2 dt^2 + \big[1-kr^2\big]^{-1}dr^2 + r^2 d\Omega^2, \\ &\text{where } kR^2 < 1, l = \frac{3GM}{R^3} \text{ and still } k = \frac{2GM}{R^3} + \frac{\Lambda}{3}. \end{aligned} \tag{31}$$

For $\Lambda = 0$ the metric reduces to the metric of a star derived by Carroll [5]. Moreover, this metric coincides with the Schwarzschild metric at $r = R$, as it should.

For $kR^2 > 1$, the square root becomes imaginary as at that point the mass is so big that the sphere must be a black hole and hence a different metric has to be used. In this thesis, we will not assume that the mass clumps are that dense, just as most of the matter in our universe. Hence the case $kR^2 > 1$ can be omitted.

3 A universe consisting of mass clumps

Now that we have found the metric for a sphere with uniform density and $\Lambda \neq 0$, we can continue creating a model of a universe consisting of mass clumps. Since this universe is consisting of regions of space containing both a mass clump and vacuum surrounding it, we would like to be able to describe such a region of space by a metric.

As already required, outside the sphere the metric will simply be the Schwarzschild metric for $\Lambda \neq 0$ from equation 14. Defining the Schwarzschild metric as $g^S_{\mu\nu}$ and defining the metric inside a uniform sphere from equation 31 as $g^I_{\mu\nu}$, we can define a new combined metric for both $r < R$ and $r > R$ using the Heaviside step function:

$$g^C_{\mu\nu} = [1 - \Theta(r - R)] \cdot g^I_{\mu\nu} + \Theta(r - R) \cdot g^S_{\mu\nu} \tag{32}$$

This metric will be referred to as the *individual metric*. Upon closer inspection, we find that actually only the tt and rr components differ inside and outside the sphere. But that is not the case for the $\theta\theta$ and the $\phi\phi$ components. Hence it is convenient to continue using an alternative but more useful and general shape of $g^C_{\mu\nu}$, being

$$g^C_{\mu\nu} = \text{diag}(g_{tt}, g_{rr}, r^2, r^2 \sin^2\theta), \tag{33}$$

in which g_{tt} and g_{rr} are different for $r < R$ and $r > R$.

3.1 Going to Cartesian coordinates

Since we are going to define the metric of our toy universe in Cartesian coordinates, let us first derive what the individual metrics are in Cartesian coordinates. For this we use the definition of a coordinate transformation:

$$g_{\alpha\beta} = \frac{\partial x^\mu}{\partial x^\alpha} \frac{\partial x^\nu}{\partial x^\beta} g_{\mu\nu} \tag{34}$$

We demanded our universe to be static and hence our spatial coordinates do not depend on time. Consequently all derivatives of the spatial coordinates w.r.t. x^0 equal zero. Hence g_{tt} has the same form in Cartesian coordinates, apart from having to write r in terms of x, y and z. However, the meaning of the modified radial coordinate r introduced in section 2, is of course different from the coordinate r that is normally used in a spatial coordinate transformation. More about this can be found in appendix A. For now we can simply continue with our transformation as if there is nothing special about our r, since our conclusion should not depend

on the chosen coordinate system. Hence we can simply use the following standard definitions for going from spherical to Cartesian coordinates:

$$r = \sqrt{x^2 + y^2 + z^2} \qquad \theta = \arctan \frac{\sqrt{x^2 + y^2}}{z} \qquad \phi = \arctan \frac{y}{x} \tag{35}$$

For ease and clarity, from this point onward r is not written out in Cartesian coordinates, hence e.g. $\partial_y r = \frac{y}{r}$. Besides, the $\phi\phi$ component can now be written down more conveniently as $g^C_{\phi\phi} = r^2 \sin^2\theta = x^2 + y^2$.

Next, we only need to transform the spatial coordinates of $g^C_{\mu\nu}$. Therefore, we need to determine the components of the inverse Jacobian matrix for going from spherical to Cartesian coordinates.

$$J^{-1} = \begin{pmatrix} \partial_x r & \partial_y r & \partial_z r \\ \partial_x \theta & \partial_y \theta & \partial_z \theta \\ \partial_x \phi & \partial_y \phi & \partial_z \phi \end{pmatrix} = \begin{pmatrix} \frac{x}{r} & \frac{y}{r} & \frac{z}{r} \\ \frac{xz}{r^2\sqrt{x^2+y^2}} & \frac{yz}{r^2\sqrt{x^2+y^2}} & \frac{-(x^2+y^2)}{r^2\sqrt{x^2+y^2}} \\ \frac{-y}{x^2+y^2} & \frac{x}{x^2+y^2} & 0 \end{pmatrix} \tag{36}$$

Performing the coordinate transformation and again leaving r as it is, gives us a convenient notation for the spherically symmetric individual metric inside a cube $g^C_{\mu\nu}$ in Cartesian coordinates:

$$\begin{aligned} g_{tt} &= g_{tt} \\ g_{xx} &= \frac{x^2}{r^2} g_{rr} + \frac{y^2 + z^2}{r^2} = \frac{x^2}{r^2}(g_{rr} - 1) + 1 \\ g_{yy} &= \frac{y^2}{r^2} g_{rr} + \frac{x^2 + z^2}{r^2} = \frac{y^2}{r^2}(g_{rr} - 1) + 1 \\ g_{zz} &= \frac{z^2}{r^2} g_{rr} + \frac{x^2 + y^2}{r^2} = \frac{z^2}{r^2}(g_{rr} - 1) + 1 \\ g_{xy} &= \frac{xy}{r^2}(g_{rr} - 1) = g_{yx} \\ g_{xz} &= \frac{xz}{r^2}(g_{rr} - 1) = g_{zx} \\ g_{yz} &= \frac{yz}{r^2}(g_{rr} - 1) = g_{zy} \end{aligned} \tag{37}$$

3.2 Designing a universe

Now we want to define a toy universe containing mass clumps by using their corresponding metric from equation 37. As it is impossible to perfectly model the real universe, we will create a more simplistic model. It should however still satisfy the assumptions that our universe is homogeneous at large scales. Moreover, this toy universe should still be isotropic and we should still be able to model it as a perfect fluid. In that way we can compare our model to the Friedmannian model and focus on the effects of inhomogeneity at small scales. In order to facilitate this comparison, we require our universe to be static. Consequently, the metric of our toy universe will be time independent and hence it will not contain a scale factor. Furthermore, for simplicity all the mass clumps will have the same values for M and R. Of course Λ will be the same throughout the entire universe.

To satisfy homogeneity and isotropy at large scales, we position infinitely many spheres on a grid, such that the resulting metric is periodically invariant. A visualisation of this set up can be found in figure 1. As you can see, this periodic placement of spheres is equivalent to stacking infinitely many cubes in all three directions. This causes the metric contribution inside all cubes to be exactly the same.

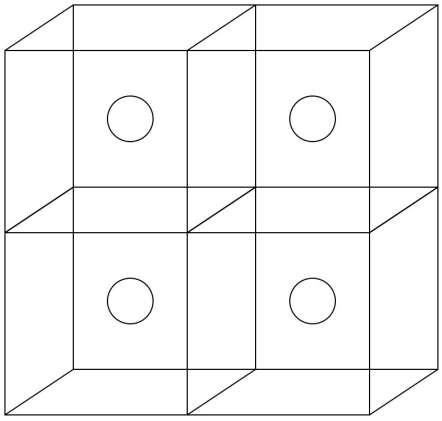

Figure 1: *A visualisation of how the spheres are periodically placed, by using a stack of cubes with spheres in the middle of them.*

Unfortunately, there is no convenient way to derive an exact solution for the total metric of this toy universe. Also, one cannot simply add two individual metrics of two neighbouring spheres as the metric near one sphere would depend on the other sphere. Nonetheless, to start with, we will anyway define the total metric to be

an infinite sum of individual metrics. However, simply taking this infinite sum is problematic, since consequently infinitely many metrics act on each point in space. Hence we would like to make sure that inside a certain cube only the metrics of the nearest neighbouring spheres contribute to the total metric inside that cube.

We do not want to simply turn off the individual metric of one sphere, when crossing the edge of the cube, and then turn on the metric of the adjacent sphere. This discontinuity causes non-existing second derivatives of the total metric at the edge of the cube. However, we will need these second derivatives for the Ricci tensor in order to be able to plug the total metric in the EFE. Hence we will apply a function, that we will call the *transition function* $f(x)$, to each individual metric, once for each direction. This function makes sure that the contribution of the metric due to one sphere smoothly vanishes inside the adjacent cube when passing the edge of the cube.

The total metric of our toy universe will be defined as:

$$\tilde{g}_{\mu\nu}(x,y,z) = \sum_{n_i=-\infty}^{\infty} g^C_{\mu\nu}(x_{n_1}, y_{n_2}, z_{n_3}) f(x,n_1) f(y,n_2) f(z,n_3) \tag{38}$$

The individual metric $g^C_{\mu\nu}$ from equation 37, is the metric corresponding to a certain cube, hence the C in the superscript. The coordinate $x_{n_1} = x - n_1 d$ has been used for periodically positioning the spheres, which are all located in the middle of a cube having width d. Using this definition, the positions of the spheres, defined using the three integers n_1, n_2 and n_3, are $(n_1 d, n_2 d, n_3 d)$. All three integers can admit values between $-\infty$ and ∞.

3.3 Determining the transition function

Normally, the metric near one sphere would be dependent on the sphere in the adjacent cube. In this simplified model, we would like to omit having to adjust the metric near one sphere due to adjacent spheres. Hence we assume that the effects of a sphere on the metric near a neighbouring sphere is negligible. Consequently, we require that inside each cube, there is effectively a region of space in which only the metric from the sphere of that cube is active. The transition function makes sure that all other individual metrics do not contribute to the total metric in that region of space.

In between two neighbouring spheres, the transition function smoothly transforms the metric of one sphere into the metric of the other. In that region it would

be strange to suddenly let one metric contribution vanish, while the other has not yet appeared. Hence we require that the transition function is defined such that effectively exactly one metric is contributing to the total metric at each point in space.

As you can see in equation 38, the transition function is applied to each individual metric three times, once for each direction. The combination of the three transition functions can now be called the *weight factor* of an individual metric as the sum of all weight factors is always equal to one. This factorisation of the weight factor in the three directions makes it easier to define the actual function for f, since in that case you only need to look at the two sides of the cube in one direction. A visualisation of the setup is shown in figure 2.

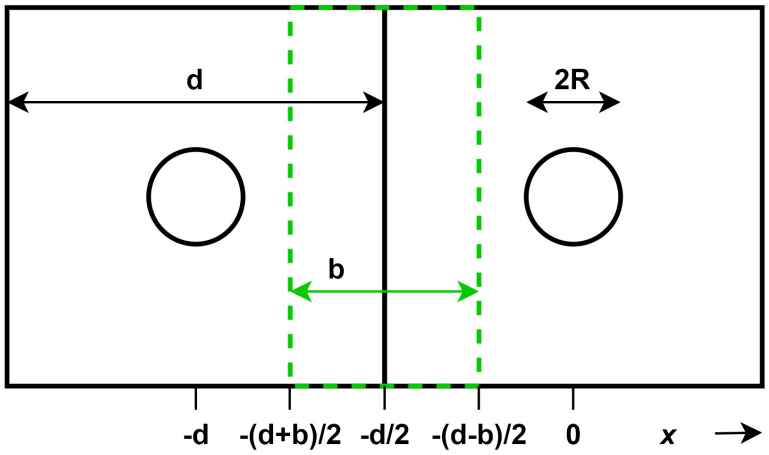

Figure 2: *A 2D representation of our definitions of the width of the border region b and the width of the cube d, using the cross section of only two cubes. Namely the zeroth cube located at (0,0,0) and a neighbouring cube located at (-d,0,0). The green dashed rectangle indicates the border region, which is the region in which the transition function acts. $2R$ is of course the diameter of the sphere.*

We will define a transition function that slowly neglects the effects of one metric and clears the path for another over a certain distance b. The region in which this function does so will be called the *border region*. For simplicity, we want the transition function to not influence the metric inside the spheres. With d being the width of a cube (and thus the distance between two spheres) and $2R$ being the diameter of a sphere, we require $b < d - 2R$.

Let us now be more specific about the values the transition function f will take. Outside the cube to which f is applied and more specifically outside the border region, extending a distance $\frac{1}{2}b$ into the adjacent cube, the effect of the metric should vanish, i.e. $f = 0$. The function at the outer edge of the border region should then start with zero, i.e. for the left side of the zeroth cube $f(-\frac{1}{2}(b+d), 0) = 0$. Then this function smoothly rises from zero to one at the other side of the border region, i.e. $f(\frac{1}{2}(b-d), 0) = 1$. Inside the cube and meanwhile outside the border regions, the function remains one, meaning that only the individual metric of that cube is active. On the other side of the cube inside the border region, the function should decrease again in exactly the same way from 1 to 0, such that $f(x)$ is symmetric around the centre of the cube in all directions.

At this point we will define the transition function to be as follows:

$$f(x, n) = S(x - nd) \cdot [1 - S(x - \{n + 1\}d)] \tag{39}$$

Here $S(x)$ is a function going smoothly from 0 to 1 around the edges of a cube over a distance b. The left term in equation 39 is responsible for the increase on the left side of the cube and the right term for the decrease on the right side of the cube. Consequently, $S(x)$ will be defined such that it increases inside the border region on the left side of the zeroth cube, whose boundary conditions have been mentioned in the previous paragraph.

To make sure that the increase on the left side equals the decrease on the right side, we demand that $1 - S(x - \{n + 1\}d) = S(-x + nd)$. For the zeroth cube, this would mean that $1 - S(x - d) = S(-x)$. Since $S(x)$ is a piecewise function, this symmetry requirement can be satisfied by taking $S(x)$ to be a kind of *smooth step function*.

Moreover, we require that the metric should not suddenly start to deviate from the original metric at the border, hence the first derivative of $S(x)$ at both edges of the border region should vanish. Otherwise, a kink in the total metric would occur, causing a discontinuity or jump in the first derivative. This causes the second derivative to be undefined at the edges of the border region as a slope cannot be taken. However, we need the second derivative to be able to calculate the EFE in the end, since we need the Ricci tensor which contains second derivatives. Consequently we require that the second derivative of $S(x)$ should exist at any point in space.

This function should furthermore not be responsible for significant density contributions in the result as the most important and interesting part is the influence of the spheres, rather than the quite unphysical border regions. However, at this point we cannot account for that yet, as we cannot very well predict the eventual effect of the border region. So for now the following relatively simple function for $S(x)$ will be used, which satisfies the previously mentioned requirements:

$$S(x) = \begin{cases} 0 & \text{if } x \leq -\frac{1}{2}(b+d) \\ -2\big(\frac{1}{b}\big[x + \frac{1}{2}(b+d)\big]\big)^3 + 3\big(\frac{1}{b}\big[x + \frac{1}{2}(b+d)\big]\big)^2 & \text{if } -\frac{1}{2}(b+d) < x < \frac{1}{2}(b-d) \\ 1 & \text{if } x \geq \frac{1}{2}(b-d) \end{cases} \tag{40}$$

Its first and second derivative inside the border region are:

$$\partial_x S(x) = \frac{6}{b}\left(\frac{1}{4} - \frac{1}{b^2}\left(x + \frac{1}{2}d\right)^2\right) \qquad \partial_x^2 S(x) = -\frac{12}{b^3}\left(x + \frac{1}{2}d\right) \tag{41}$$

As can be seen, the first derivative of $S(x)$ is indeed equal to 0 at $x = -\frac{1}{2}d \pm \frac{1}{2}b$, i.e. at the edges of the border region, and the second derivative exists, as desired.

3.4 Implications of the smooth step function

We could have of course chosen many other functions fulfilling the same requirements. At this point there is not really a physical reason for a preference, so our choice is still arbitrary. One advantage of this function is that this function is relatively simple and this will likely save computation time in the end. Moreover, this function really has a beginning and an end. Hence, by choosing the right values for b, d and R, we can make sure that $S(x)$ does not act on the metric inside the sphere, but only on the Schwarzschild metric, which again saves computation time. Other effects of this function, that make this definition a good first trial function, will become clear in the rest of this section.

As required, due to our definition of $f(x)$, the sum of just two transition functions (without its corresponding individual metric), inside the border region of two adjacent cubes, adds up to 1. This can be shown by looking at the remaining transition functions of two adjacent cubes, inside their corresponding border region:

$$\begin{aligned} &f(x, n-1) + f(x, n) \\ &= S(x - \{n-1\}d)[1 - S(x - nd)] + S(x - nd)[1 - S(x - \{n+1\}d)] \\ &= 1 \cdot [1 - S(x - nd)] + S(x - nd) \cdot 1 = 1 \end{aligned} \tag{42}$$

Even when the transition functions of other directions are applied, and when looking at border regions in which 4 or 8 transition functions overlap, the sum of the weight factors adds up to 1. Hence $f(x)$ makes sure that effectively no more than one metric is acting on each point in space, as required. Of course, outside the border region only one of all the weight factors equals 1, causing only one metric to be active there.

It is also good to note that the transition functions of two adjacent cubes are each others mirror functions, when placing a mirror at the edge between the two cubes. That is because $S(x-d) = 1 - S(-x)$ and thus $\partial_x S(x-d) = -\partial_x S(-x)$. In other words, if you would shift $S(x)$ such that the transition is centred at $x = 0$, rather than $x = -d/2$, the relations $S(x) = 1 - S(-x)$ and hence $\partial_x S(x) = -\partial_x S(-x)$ can be proven. Hence the derivative of two transition functions of two adjacent cubes are also mirrored around the centre of the border region and they are of opposite sign.

These properties actually already follow from our previously mentioned requirements, but it is useful to explicitly show them anyway. In that way, we are able to more easily get a grasp of what the components in the EFE should look like, using our total metric. This will even help us simplify calculations in the upcoming chapters.

3.5 Symmetries in the EFE

Let us now look at the effects of $S(x)$ on the total metric. For that we will first look at the effects of the spherically symmetric definition of a distance, after which we will see that these effects also apply to the individual metric in Cartesian coordinates. Having $ds^2 = g_{\mu\nu} dx^\mu dx^\nu$ and knowing that ds^2 is spherically symmetric, we see for $\mu = \nu$ that $dx^\mu dx^\nu$ is symmetric in all directions and hence $g_{\mu\nu}$ must be so too. However, simply dx^μ is antisymmetric with respect to the plane orthogonal to the axis denoted by μ. In the upcoming paragraphs, we will use a simpler way of saying the latter, namely: "dx^μ is antisymmetric in the direction of μ." So if $\mu \neq \nu$, then $dx^\mu dx^\nu$ is an odd function only in the direction of μ and ν and hence $g_{\mu\nu}$ must be so too, such that ds^2 is symmetric again in all directions.

We already know that the components g_{rr} and g_{tt} of the individual metric are spherically symmetric around the centre of the cube. Furthermore, the transition function $f(x)$ is symmetric around the centre of the cube in all three directions. Then one can quickly observe the following two properties by looking at the individual metric in Cartesian coordinates $g^C_{\mu\nu}$ from equation 37:

Firstly, the components on the diagonal are indeed all symmetric functions in the direction of x, y and z around the centre of the cube. Consequently, when applying the weight factor, the on-diagonal components of the total metric $\tilde{g}_{\mu\nu}$ is also symmetric in the three directions around the centres of all the cubes. On top of that, it is symmetric around the planes between the cubes in all three directions.

Secondly, the off-diagonal components of $g^C_{\mu\nu}$ are indeed antisymmetric in the directions denoted by its indices around the centres of the cubes. So for instance g^C_{xy} is antisymmetric in the direction of x and y, and symmetric in z. Consequently, those components of the total metric $\tilde{g}_{\mu\nu}$ are also antisymmetric in the directions denoted by its indices around the centres of the cubes, but symmetric in the direction that is not denoted by its indices. On top of that, those components transition smoothly from a certain value at the left side of the border region to minus that same value at the right side of the border region. Hence, the off-diagonal components of the total metric are antisymmetric in the direction denoted by its indices around all the planes between the cubes, but again symmetric in the direction that is not denoted in its indices.

Moreover, one can see that the derivative of a symmetric function will result in an antisymmetric derivative. For instance, this implies that the total metric components for which $\mu = \nu$ will have antisymmetric derivatives around the border and the sphere centres in the direction of the chosen derivative. If one would extrapolate these symmetries even further to the other symbols needed for the EFE, one would eventually come to the following conclusion: The function of the symbol (e.g. $\Gamma^{\alpha}_{\beta\gamma}$) is symmetric/antisymmetric in the direction of e.g. α if there is an even/odd number of indices equal to α present in that symbol.

Consequently, the Ricci scalar, which has no indices, is symmetric in all three directions. Moreover, the entire EFE is symmetric around the planes between the cubes and around the centres of the cubes in all three directions for $\mu = \nu$, and antisymmetric in the direction denoted by its indices for $\mu \neq \nu$. As such, the tt component of the stress-energy tensor is symmetric around both the centres of the cube and the border region, in all three directions. The latter is a useful property in simplifying the upcoming steps in the next sections.

4 Sifting the total metric

Now that we have obtained a well defined total metric, we would like to be able to actually do something with it. In the end, as already mentioned in the introduction, we would like to compute the average density of our toy universe and compare this to what density the Friedmann model would expect for our toy universe. But in order to get there, some tricks have to be performed, which will be elaborated in the rest of this chapter.

4.1 Defining usable regions

In this section, we are going to split up the total metric into a few more practical metrics. Earlier, we have made sure that our toy universe is homogeneous at large scales, since we required all cubes to look exactly the same. Consequently, we only have to look at the metric inside one cube and with that we know exactly what the metric looks like in all the other cubes. Hence, from now on we only consider the metric inside the zeroth cube, which is positioned at the origin.

Moreover, due to our piecewise transition function, the zeroth cube can be split up into numerous discrete regions. In total, there are five different kinds of regions and hence we only need to choose and consider five specific regions and their corresponding metrics. These five different regions together are then sufficient to describe the entire universe. Let us first define the five regions that have been visualised in figure 3.

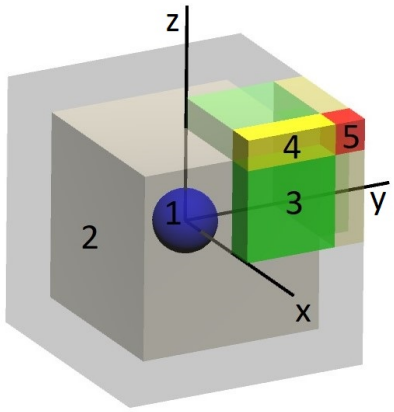

Figure 3: *A 3D representation of the five different regions inside a single cube that are enough to represent our entire toy universe.*

1. First of all, we have the region inside the sphere having radius R, which is positioned at the origin.

2. Then we have the region outside the sphere and outside the border region, in which simply the Schwarzschild metric operates. Only the first octant (i.e. $x, y, z \in [0, \frac{1}{2}(d-b)]$) has been evaluated, to save computation time.

3. We have regions in which two metrics overlap. The region representing such an overlap region is chosen to be the border region of the zeroth cube (0,0,0) and its neighbouring cube (1,0,0). Hence, the total metric is composed of two Schwarzschild metrics on which one transition function for the x-direction is acting, as the transition functions in the other two directions are equal to 1. Furthermore, we only look at the first octant of the zeroth cube again, causing this third region to be described by the coordinates:
   $x, y, z = [\frac{1}{2}(d-b), \frac{1}{2}d], [0, \frac{1}{2}(d-b)], [0, \frac{1}{2}(d-b)]$.
   As can be seen more easily in figure 3, this third kind of volume is present three times in the first octant. Hence the third region is present $3 \times 8 = 24$ times in the zeroth cube.

4. Also, we have the regions in which four metrics overlap. Hence, the total metric is the sum of four Schwarzschild metrics on which two smooth step functions are acting per term, for instance the ones in the x and z direction of the first octant depicted in figure 3. Hence this particular region is described by the coordinates:
   $x, y, z = [\frac{1}{2}(d-b), \frac{1}{2}d], [0, \frac{1}{2}(d-b)], [\frac{1}{2}(d-b), \frac{1}{2}d]$.
   This kind of volume is also present 24 times in the cube.

5. Lastly, we have regions in which eight metrics overlap. Consequently, the total metric is the sum eight Schwarzschild metrics on which three smooth step functions are acting per term. For the first octant this region corresponds to:
   $x, y, z = [\frac{1}{2}(d-b), \frac{1}{2}d], [\frac{1}{2}(d-b), \frac{1}{2}d], [\frac{1}{2}(d-b), \frac{1}{2}d]$.
   This kind of volume is present only 8 times in the cube.

For the latter three regions, we only need to look at parts of the border region, as the other parts again act similarly. That is because the metric without transition functions is spherically symmetric, and the applied transition functions are alike in the x, y and z direction, as has been explained in section 3.5. So, for instance the border region in which 8 metrics overlap in the first octant (region 5) is the same as similar overlap regions in the other octants, up to a reflection in a certain plane. Knowing the metric of a region, we can simply extrapolate its properties to the rest

of the border region if this is needed.

In this way we can choose a part of the border region where some of the smooth step functions are equal to zero or one, causing the corresponding metric to be less extensive. Consequently, we will be able to take for instance the inverse of each separate metric with much greater ease than taking the inverse of the total metric (being an infinite sum of individual metrics with a certain weight factor). Not only does this approach save time in describing the entire cube, but it also saves a lot of computation time in the end.

4.2 Computing the EFE's

Now that we have defined those five different regions, we would like to obtain the corresponding EFE per region, which together can describe the properties of our entire toy universe. For that we will first need the inverse metric of all those regions, such that we can calculate the Christoffel symbols, and so on.

The inverse metric of the first and second region can still be obtained algebraically with relative ease. Having the definition of the spherically symmetric metrics in Cartesian coordinates, defined in equation 37, we can take its matrix inverse to obtain the inverse metric. After some rewriting, the inverse metric for the first and second region result to be:

$$\begin{aligned}
g^{tt} &= g_{tt}^{-1} \\
g^{xx} &= \frac{y^2+z^2}{r^2}(1-g_{rr}^{-1}) + g_{rr}^{-1} \\
g^{yy} &= \frac{x^2+z^2}{r^2}(1-g_{rr}^{-1}) + g_{rr}^{-1} \\
g^{zz} &= \frac{y^2+x^2}{r^2}(1-g_{rr}^{-1}) + g_{rr}^{-1} \\
g^{xy} &= -\frac{xy}{r^2}(1-g_{rr}^{-1}) \\
g^{xz} &= -\frac{xz}{r^2}(1-g_{rr}^{-1}) \\
g^{yz} &= -\frac{yz}{r^2}(1-g_{rr}^{-1})
\end{aligned} \tag{43}$$

The last three regions, however, are not described by spherically symmetric metrics anymore and hence the inverse metric cannot be calculated using equation 43. Fortunately, inside these overlap regions, the corresponding metrics have taken a

much more comprehensible shape already. That is because $S(x)$ in such a region does not need to be described by a piecewise function anymore. However, finding the inverse metric will still take some time as one will have to determine the matrix inverse of the metric tensors and this will likely not result in such an elegant solution as before. Moreover, in order to obtain the necessary components of the EFE, i.e. the Ricci tensor and scalar, one would have to spend lots of time calculating these components.

Hence from now on, everything has been computed in a computer program, which is appended to this thesis. For some extra elaborations on this program (besides the comments in the file), you might want to have a look at the appendix, as some not so straightforward steps and tricks have been taken in order to save computation time. The general idea is still important to mention now as this determines the result. Hence we will briefly describe what steps we have taken.

The steps in obtaining the time component of the stress-energy tensor are straightforward. Having the metrics and the inverse metrics inside and outside the sphere (regions 1 and 2), we only need to compute the inverse of the metrics of the border regions (regions 3, 4 and 5) by matrix inversion. Then the Christoffel symbols and subsequently the Ricci tensor and scalar can be computed, for each of the five regions separately. Finally, one can calculate the stress-energy tensor by plugging in the components in the left hand side of the EFE as defined in equation 1.

4.3 The average mass density of the universe

The components of this stress-energy tensor from all the regions together will not resemble a perfect fluid anymore inside the cube as both the pressure and density are different throughout the five different regions. However, one may argue that when looking at the universe as a whole at large scales, such that one cannot distinguish the individual spheres anymore, then the universe may be treated as homogeneous and isotropic again. Since we set up our spheres to be static and non-interacting, we can consider our toy universe as a whole at large scales to contain a perfect fluid.

The latter remark is consistent with the assumptions forming the basis of the Friedmann equations. As many years of research have already shown, these assumptions about the universe are able to explain our observations very well. Hence, despite the fact that our model is different on small scales, it should in the end have some concordance with the standing Friedmann model at large scales. Consequently, it is

not so strange to consider our modelled universe to be a perfect fluid at large scales. Yet we have to investigate what the effects of inhomogeneity on small scales are.

The assumption of our modelled universe being a perfect fluid is very useful, since we can now determine the average mass density of our toy universe and compare this to the mass density we would have expected for our model using the Friedmann equations. To get the average mass density of our toy universe, we again only have to look at one cube and determine its average mass density. With that we directly know the average mass density of our entire modelled universe.

Let us now find out how to get this average mass density. By using the definition of the stress-energy tensor of a perfect fluid from equation 11, the following equation holds for the time component of the stress-energy tensor of a perfect fluid:

$$\rho = -\frac{T_{tt}}{g_{tt}} \tag{44}$$

The region inside the sphere is a perfect fluid already, as this was demanded at the beginning. By calculating the needed components of the EFE one can find out that the time component of the stress-energy tensor divided by $-g^I_{tt}$, results in the constant density of the sphere, as expected.

The density of the second region, resulting from the Schwarzschild metric, will vanish after performing the same steps. This on the one hand seems very logical as we are looking at a vacuum. But on the other hand, one might expect to see a density resulting from the cosmological constant, being interpretable as the energy density of the vacuum. However, this is not the case, since we did not put the Λ term of the EFE (equation 1) into the stress energy tensor.

The mass densities resulting from the metrics of the different border regions happen to be dependent on the location inside the border region. Hence we have to average over the border regions in order to obtain the average density. This averaging can be done by taking the integral of the densities over the volume of the specific region to get its total mass, and then divide by its volume. Since we are averaging in a curved space, we have to take the curvature into account, after which we obtain the correct mass, volume, and with that the average mass density. To this end, we have to use the following integration measure:

$$dV = \sqrt{|g_{ij}|}d^3x. \tag{45}$$

Here $|g_{ij}|$ is the determinant of the spatial components of the metric, hence the ij subscript. Sometimes it is denoted as $\mathrm{Det}(\tilde{g})$, but we already have another use of $\tilde{g}$. The mass resulting from the n^{th} region with volume V_n is then obtained as:

$$\overline{M}_n = \int_{V_n} \rho_n dV = \int_{V_n} \rho_n \sqrt{|g_{ij_n}|} d^3x \tag{46}$$

Note that this integration also has to be performed for the first region to obtain the real mass of the sphere. The density still is constant throughout the sphere in the coordinates in which the constant density has been defined. However, the curvature arising from the mass of the sphere and the cosmological constant causes the actual mass inside the sphere $\overline{M}_1$ to be different from the quantity M that has been put into for instance the Schwarzschild metric.

We then choose to divide the mass by V_C, the volume of the entire cube, to obtain the average mass density. In that way, the average mass density is not the mass density of that component inside its own region, but it really is the mass density inside the cube. Thereby, the average mass density $\overline{\rho}_n$ directly is the average mass density inside the universe, resulting from that n^{th} region:

$$\overline{\rho}_n = \frac{\overline{M}_n}{V_C} \tag{47}$$

The volume of the n^{th} region is defined by:

$$V_n = \int_{V_n} \sqrt{|g_{ij_n}|} d^3x \tag{48}$$

Since only a part of each of the kinds of regions has been used, we have to multiply the obtained volume by a certain factor in order to obtain the entire volume of such a kind of region inside a cube. For instance in the first octant, the third region is present in two other orientations, also having a volume V_3. And since there are eight octants inside a cube, the total volume $V_{3_{tot}}$ resulting from the third region is: $V_{3_{tot}} = V_3 \cdot 3 \cdot 8$. Consequently the total volume of the cube can be written down as:

$$V_C = V_1 + 8V_2 + 24V_3 + 24V_4 + 8V_5 \tag{49}$$

Similarly, the masses of the sphere $\overline{M}_I$ and the border region inside a cube $\overline{M}_B$ are $\overline{M}_I = \overline{M}_1$ and $\overline{M}_B = 24\overline{M}_3 + 24\overline{M}_4 + 8\overline{M}_5$ respectively. Consequently, the average mass density of the universe is

$$\overline{\rho} = \overline{\rho}_I + \overline{\rho}_B, \text{ where } \overline{\rho}_I = \frac{\overline{M}_I}{V_C} \text{ and } \overline{\rho}_B = \frac{\overline{M}_B}{V_C}. \tag{50}$$

Here $\overline{\rho}_I$ is the average mass density resulting from the mass clumps and $\overline{\rho}_B$ is the mass density resulting from the border regions.

4.4 Expectations from the Friedmannian model

For a homogeneous perfect fluid with mass density ρ, constant spatial curvature and $\Lambda \neq 0$, the first Friedmann equation [7] is given by:

$$H^2 = \left(\frac{\dot{a}}{a}\right)^2 = \frac{8\pi G}{3}\rho + \frac{\Lambda}{3} - \frac{\kappa}{a^2} = \frac{8}{3}\pi G(\rho + \rho_{vac}) - \frac{\kappa}{a^2} \tag{51}$$

This is only one of the two Friedmann equations, but this is the only one we will need right now. In this equation a represents the scale factor, which indicates the size of the universe, whereas $\dot{a}$ represents the velocity at which the universe is expanding. Together they form the expansion rate $\dot{a}/a$, better known as the Hubble constant, H. The Hubble constant at present time is known as the Hubble parameter H_0, whose measured values are inconclusive. In our model we are trying to see whether this equation still holds, or whether extra contributions to the expansion rate arise due to mass clumping.

In order to check if the first Friedman equation will hold for our modelled universe, we will have to plug in the parameters corresponding to our toy universe. Firstly, we assumed our toy universe to be static, causing the expansion rate $\dot{a}$ to equal zero. Secondly, there is a curvature term in the Friedmann equation, described by κ. The curvature of our model universe is equal to zero, which we will elaborate using the following thought experiment.

Imagine a photon travelling along the border exactly between two cubes. Since the influence of both spheres cancel each other out, the photon must be travelling in a straight path. Due to periodicity, any such photon would be travelling in a straight line anywhere in the universe. This causes us to have a flat universe, i.e. $\kappa = 0$. Even when the photon is not travelling exactly between the two cubes, the photon will on average travel in a straight line on large scales, as it is randomly distorted by the local curvature due to the mass clumps. We omit the case in which the photon scatters on a sphere, as this has nothing to do with the curvature of the universe.

Having $H = 0$ and $\kappa = 0$, the first Friedman equation reduces to

$$\frac{8\pi G}{3}(\rho + \rho_{vac}) = 0, \tag{52}$$

Hence one can conclude for our model that if the Friedmann equation would hold, the average energy density of our toy universe should be equal to minus the vacuum energy density and hence $\overline{\rho} = -\rho_{vac}$. Consequently, if $\Lambda = 0$, then $\overline{\rho}$ should exactly equal zero.

You might already expect at this point that the computer program will return a non-zero average energy density for $\Lambda = 0$ using the following reasoning. The model consists of mass clumps with a certain density and outside the spheres there is a vacuum described by the Schwarzschild metric, having a zero energy density. Also there is the nonphysical transition function acting on the Schwarzschild metric in the border region, whose width can at this moment be chosen arbitrarily. Hence its contribution to the density can be anything, but it is not logical that this function will exactly compensate for the mass inside the spheres. However, the latter is not trivial and hence we must check if not somehow in the end the total average density will indeed be zero, causing our model to be in line with the Friedmannian model.

As just mentioned, the width of the border region can yet be anything. The only requirement is that the energy density contribution from the rather unphysical border region should be minimal, compared to that of the rest of the more physical volume. Or more precise, the energy density resulting from the border metric should be small compared to that from the mass clumps. Requiring this, you might already want to conclude that the total energy density is not zero. However, we do not know if we are able to minimise its contribution at this point. If there is no dependence on the width of the border, it may even be possible that the density of the border always exactly cancels the density of the mass clumps. In order to exclude this possibility for our model we should have a look at the dependence of the total average energy density on b.

In conclusion, we only need to check if the total average mass density does not always satisfies the following equation: $\overline{\rho} = -\rho_{vac}$. Besides, we would like to be able to minimise the contribution of the unphysical border region. In that case we can say with more confidence whether we have made a physical model that is not in line with the Friedmannian model.

5 Results

5.1 Clarification of the choice of input values.

Now that we have a method to compute $\overline{\rho}$, we would like to choose some sets of input values such that we can investigate the dependence on the different parameters of the model. We will need these dependencies to see if we are able to minimise the contribution of the border region. The only parameters appearing in the total metric that we can adjust are the mass of the sphere M, its radius R, the cosmological constant Λ, the width of the cube d and the width of the border region b.

Before we choose different sets of those input values, please note that we have used cosmological units in the computer program, such that $G = c = 1$. Hence we will choose values for the mass of the sphere by actually choosing a value for the combination GM/c^2, rather than simply M. In the results presented in tables 1 and 2 we therefore both give the exact input value for GM/c^2 in meters and the rounded value for M in kilograms. The latter value will be given as it makes the comparison to the output values easier.

In the computer program we are unable to choose realistic values for the input values M, R and Λ as the limited precision of floats causes the numerical errors to become too large. Hence we choose the terms occurring in our metrics to have about the same order of magnitude, i.e. $1 \sim 2GM/c^2R \sim \Lambda R^2/3$, which in addition saves computation time. The consequences of choosing such unrealistically large numbers will be discussed in section 5.3.

Now we will quickly elaborate why we have chosen some sets of input values. As a first step, we will choose $R = 1$ m in all calculations and we will vary M, Λ, b and d to investigate their effects.

First of all, we would like to test the effects of changing b, d and M in the simple case in which $\Lambda = 0$. This case takes less computation time and will thus be easier to test on. Of course we have to watch out for all the singularities and extreme behaviours of the Schwarzschild metric. So we have to choose M such that we are not dealing with a black hole. In the case that $\Lambda = 0$, we can do so by positioning the Schwarzschild radius within the sphere, i.e. $2GM/c^2 < R$. Having $R = 1$ m, we will simply choose $GM/c^2 = 1/6$ m. Furthermore, we would like to test what the effects are of adjusting the properties of the border, hence $d = 4$ m & $b = 1/2$ m and

$d = 4$ m & $b = 1/32$ m have been chosen as well as $d = 8$ m & $b = 1/32$ m. The corresponding results can be found in table 1.

Next it would be interesting to observe the effects of dark energy in our model. However, when choosing $\Lambda \neq 0$, we have to avoid a second singularity, namely the de Sitter cosmological horizon, which occurs at large radii. Hence we have to choose Λ and M, such that this horizon lies outside the cube. Moreover, it would be interesting to choose a value for Λ such that the density of the sphere equals the dark energy density, i.e. $\rho = \rho_{vac}$, as in our real universe the overall matter energy density is currently about the same as the vacuum energy density. However, when having e.g. $GM/c^2 = 1/6$ m & $d = 8$ m & $b = 1/32$ m, it is not possible to choose a Λ such that $\rho = \rho_{vac}$ due to the singularities. Hence the value of $\Lambda = 1/18$ m^{-2} has been chosen, with the aim that ρ_{vac} is at least of the same order as ρ ($\rho = 18\rho_{vac}$), such that the effects of the cosmological constant are still noticeable in the results. For comparison, it would anyhow still be interesting to have a situation in which $\rho = \rho_{vac}$ does hold. Hence having $\Lambda = 1/18$ m^{-2}, we have to choose $GM/c^2 = 1/108$ m in that case. Then again the two cases $d = 4$ and 8 m will be tested. This gives us three cases for $\Lambda \neq 0$, which can be found in table 2.

We did not compute more than three results for $\Lambda \neq 0$ simply because those computations took about twice as long as those for $\Lambda = 0$, which already took a few days. Yet we will be able to perform an investigation of the results for $\Lambda \neq 0$ that is sufficient for our goals, also partially because we have added two more cases for $\Lambda = 0$ m^{-2} & $GM/c^2 = 1/108$ m, which we can then compare to the $\Lambda = 1/18$ m^{-2} cases.

5.2 Comparison to the Friedmannian model

Results in the case of $\Lambda = 0$ m^{-2}

Let us first show and discuss the results in the case that $\Lambda = 0$, as it consists of the most extensive set of output values. Moreover it is easier to interpret as we do not yet have to take dark energy into account. As a reminder, in this case we especially would like to see if $\overline{\rho}$ always equals zero or not.

Table 1: *In this table the input values $R = 1$ m and $\Lambda = 0$ m^{-2} have been used. Here $\overline{M}_I$ and $\overline{M}_B$ are the integrated masses inside the sphere and the border region of one cube, respectively. V_C is the volume of the cube. The average mass density in the universe resulting from the mass clumps is $\overline{\rho}_I = \overline{M}_I/V_C$ and that resulting from the border region is $\overline{\rho}_B = \overline{M}_B/V_C$. Then the sum of $\overline{\rho}_I$ and $\overline{\rho}_B$ gives the average mass density of our toy universe $\overline{\rho}$. As can be seen, none of the average mass densities equal zero. Moreover, there are some useful dependencies on the input parameters, as will be discussed in the text. Note that we have not shown any numerical errors, as all the errors are (way) smaller than the numbers presented in the table. Hence we choose to write down the values using only four digits, which is the biggest number of digits for which no error occurs.*

Input	GM/c^2 (m)	1/6			1/108	
	M (10^{23} kg)	2244			124.7	
	d (m)	4		8	4	8
	b (m)	1/2	1/32	1/32	1/32	1/32
Output	$\overline{M}_I$ (10^{23} kg)	2838	2838	2838	126.1	126.1
	$\overline{M}_B$ (10^{23} kg)	-2571	-2566	-2392	-125.5	-125.1
	V_C (m^3)	78.27	78.26	568.1	64.64	514.8
	$\overline{\rho}_I$ (10^{23} kg m^{-3})	36.26	36.27	4.996	1.951	0.2449
	$\overline{\rho}_B$ (10^{23} kg m^{-3})	-32.84	-32.78	-4.210	-1.942	-0.2430
	$\overline{\rho}$ (10^{23} kg m^{-3})	3.421	3.486	0.7859	0.008566	0.001905

In table 1, $\overline{\rho}_B$ keeps having a value being close to that of $-\overline{\rho}_I$, regardless of the values chosen for M, b and d. Hence, it is as if the transition function is in some way compensating for the mass density resulting from the mass clumps, but it does not completely succeed to do so. Consequently, none of the average mass densities equals zero in this model for $\Lambda = 0$, contradicting the expectations given by the first Friedman equation. The latter contradiction is then the result of mass clumping, as the mass in the Friedmannian model of the universe is uniformly distributed.

Let us now check that in the limit that mass clumping does not contribute to the average mass density of the universe, that $\overline{\rho} = 0$ again, such that our model is in line again with the Friedmannian model. First of all, when lowering the mass of the sphere M we see that the ratio $\overline{\rho}_I/\overline{\rho}_B$ approaches -1 for decreasing M, meaning that the border region is more easily able to compensate for the mass density arising from

the mass clumps. Consequently, as we can see in table 1, $\overline{\rho}$ decreases for decreasing M, just as expected. Even when we would compare the relative decrease of $\bar{\rho}$ with respect to for instance $\overline{\rho}_I$, i.e. $\bar{\rho}/\overline{\rho}_I$, a decrease can be observed. This decrease can be interpreted as approaching the Friedmannian model for decreasing M.

Second of all, when increasing the size of the cube d we see a decrease in $\overline{\rho}$ again. However, the ratio $-\overline{\rho}_I/\overline{\rho}_B$ increases for increasing d, meaning that the border region is less easily able to compensate for the mass density resulting from the mass clumps. Moreover, we observe an increase in $\bar{\rho}/\overline{\rho}_I$, which can be interpreted as a departure from the Friedmannian model. This means that the effects of mass clumping is more significant if the mass clumps occupy smaller fractions of space. In other words, the less homogeneous our toy universe is, the less the Friedmannian model is in line with our toy model. Even though we cannot explicitly show (using table 1) that $\overline{\rho} = 0$ again, in the limit that mass clumping does not contribute to $\overline{\rho}$, we could at least show that our model is heading towards that result when decreasing M or d.

As already mentioned, we would like to minimise the contribution of the rather unphysical border region, such that we obtain a universe in which only the more physical mass clumps determine the average density of the universe. In other words, we should check if we can minimise $|\rho_B|$ with respect to $|\rho_I|$, meaning that ρ_I is non-zero if $|\rho_B|$ is zero or small with respect to $|\rho_I|$. Fortunately, we can find out that we can indeed do so by investigating the dependencies on the different input parameters.

In table 1, it turns out that adjusting the width of the border region b barely makes a difference in the resulting $\overline{\rho}_B$ in the case that $GM/c^2 = 1/6$ m & $d = 4$ m. Yet there is a dependence on b. Namely, if b gets smaller, then the volume of the cube becomes smaller as well. Of course, $\overline{M}_I$ is independent of b, hence if b becomes smaller, then $\overline{\rho}_I$ becomes bigger. Moreover, we see that shrinking the border region causes $\overline{M}_B$ to be bigger, i.e. its absolute value gets smaller, as is thus the case for $\overline{\rho}_B$. However, again it does not change very much. So we could decrease b many orders, such that perhaps the unphysical $|\overline{\rho}_B|$ can be minimised with respect to the more physical $|\overline{\rho}_I|$. However, the dependence on b at such low values of b is unknown. Hence we do not know for sure if we can remove this unphysical mass density contribution in our model for $\Lambda = 0$ by altering b.

Fortunately, we may be able to do so by altering d, after which our model is still not in line with the Friedmannian model. It appears that for bigger d, $\overline{M}_B$ gets closer to zero from below, even though the volume of the border region gets bigger,

causing $\overline{\rho}_B$ to approach zero from below as well. Meanwhile, $\overline{M}_I$ of course remains constant for bigger d, causing $\overline{\rho}$ to remain non-zero. This would indicate that for $\Lambda = 0$ one would have to increase d drastically to be able to minimise $|\overline{\rho}_B|$ with respect to $|\overline{\rho}_I|$. One can also simply compute the ratio $-\overline{\rho}_I/\overline{\rho}_B$, which becomes bigger when increasing d from 4 m to 8 m. From this we can conclude again that one can minimise $|\overline{\rho}_B|$ w.r.t. $|\overline{\rho}_I|$ by increasing d.

This makes sense as for large distances from the sphere, the Schwarzschild metric for $\Lambda = 0$ approaches the flat Minkowski metric. Hence, if the border region is located far from the spheres, the transition function will have barely any effect on the total metric, as the individual metrics are already nearly flat. This causes $\overline{M}_B$ to approach zero, whereas $\overline{M}_I$ remains constant. However, this is not necessarily the case for $\Lambda \neq 0$ as then the Schwarzschild metric approaches the De Sitter metric, which is certainly not flat for large distances from the sphere.

Results in the case of $\Lambda = 1/18$ m^{-2}

To test if $\overline{\rho} = -\rho_{vac}$ holds, we would now like to know what the value of ρ_{vac} is for the only used value of Λ in the computations, which is $\Lambda = 1/18$ m^{-2}. Using $\Lambda = 8\pi\rho_{vac}G$, we find that ρ_{vac} should have a value of $2.977 \cdot 10^{24}$ kg m^{-3}. Hence we would like to see if $\overline{\rho} = -2.977 \cdot 10^{24}$ kg m^{-3}, which is the case if the Friedmannian model holds for $\Lambda = 1/18$ m^{-2}.

As one can see in table 2, $\overline{\rho}$ is not equal to $-2.977 \cdot 10^{24}$ kg m^{-3} in any of the three cases. The value for $\overline{\rho}$ in the case of $GM/c^2 = 1/108$ m & $d = 4$ m lies surprisingly close to that number, however, it is certainly not the same taking into account the error margins. Moreover, the cases for $GM/c^2 = 1/108$ m & $d = 8$ m and $GM/c^2 = 1/6$ m & $d = 4$ m give significant deviations. Hence we can conclude that our model for $\Lambda \neq 0$ is not (always) in line with the Friedmannian model.

Now we would like to investigate the possibility to minimise of $\overline{\rho}_B$ for $\Lambda \neq 0$ as well. In that case, the resulting $\overline{\rho}$ seem to be very sensitive to Λ as it is not naturally true anymore that $\overline{\rho}_B \approx -\overline{\rho}_I$. Moreover, a very peculiar result is that for $GM/c^2 = 1/108$ m & $d = 8$ m the mass density resulting from the border region $\overline{\rho}_B$ is positive, whereas all the other computed $\overline{\rho}_B$ are negative. Changing d from 8 to 4 m, or changing Λ from 1/18 to 0 m^{-2} causes $\overline{M}_B$ to become negative. So, when choosing an intermediate value for d or Λ, one can even make sure that $\overline{M}_B$ completely vanishes.

Table 2: *In this table the input values $R = 1$ m, $b = 1/32$ m and $\Lambda = 1/18$ m^{-2} have been used. Again $\overline{M}_I$ and $\overline{M}_B$ are the integrated masses inside the sphere and the border region of one cube, respectively. V_C is the volume of the cube. The average mass density in the universe resulting from the mass clumps is $\overline{\rho}_I = \overline{M}_I/V_C$ and that resulting from the border region is $\overline{\rho}_B = \overline{M}_B/V_C$. Then the sum of $\overline{\rho}_I$ and $\overline{\rho}_B$ gives the average mass density of our toy universe $\overline{\rho}$.*

Input	GM/c^2 (m)	1/6	1/108	
	M (10^{23} kg)	2244	124.7	
	d (m)	4	4	8
Output	$\overline{M}_I$ (10^{23} kg)	2883	127.5	127.5
	$\overline{M}_B$ (10^{23} kg)	-5164	-2216	44.87
	V_C (m^3)	85.83	69.98	779.5
	$\overline{\rho}_I$ (10^{23} kg m^{-3})	33.59	1.822	0.1636
	$\overline{\rho}_B$ (10^{23} kg m^{-3})	-60.16	-31.67	0.05756
	$\overline{\rho}$ (10^{23} kg m^{-3})	-26.57	-29.85	0.2212

Let us now check that even when $\overline{M}_B$ vanishes, $\overline{M}_I$ does not vanish. When looking at for instance the case that $GM/c^2 = 1/108$ m & $d = 8$ m in both tables 1 and 2, we see that increasing Λ, such that $\overline{M}_B$ vanishes, causes $\overline{M}_I$ to increase as well. Of course, adjusting d such that $\overline{M}_B$ vanishes, does not affect $\overline{M}_I$. Hence for a finite M and R, $\overline{M}_I$ does not necessarily become zero when $\overline{M}_B$ does, causing $|\overline{M}_B|$ to be minimizable with respect to $|\overline{M}_I|$. Consequently, $|\overline{\rho}_B|$ really is minimizable w.r.t $|\overline{\rho}_I|$ in the case that $\Lambda = 1/18$ m^{-2}, as desired.

Now we would only like to check if in the case that $\overline{\rho}_B$ vanishes, the Friedmannian model still does not hold. We can do so by again looking at the cases in which $GM/c^2 = 1/108$ m & $d = 8$ m. In both the $\Lambda = 0$ m^{-2} and the $\Lambda = 1/18$ m^{-2} case, $\overline{\rho}$ is positive. For the intermediate value of Λ, such that $\overline{M}_B$ becomes zero, $\overline{M}_I$ remains positive and hence we do not expect $\overline{\rho}$ to suddenly become negative. When having found this positive Λ and thus a positive ρ_{vac}, we do not expect the equation $\overline{\rho} = -\rho_{vac}$ to hold. Consequently, it is possible to create a universe (using this model) in which $|\overline{\rho}_B|$ is minimised, while this universe is still not in line with the Friedmannian model.

In other words, for $\Lambda \neq 0$, we are able to create a universe, in which not the unphysical border region, but only the mass clumps in combination with the dark energy, contribute to the average mass density of the universe. And such a universe does not need to be in line with the Friedmannian model. Since we were not able to predict beforehand for what input values we could minimise $\overline{\rho}_B$, it is good to see that there is at least a possibility to do so.

In short: our model is not in line with the Friedmannian model for any of our chosen set of input values. However, our model does seem to approach the Friedmannian model if M or d is decreased, causing our toy universe to become more homogeneous. Moreover, for at least some sets of input values we can create a universe in which the unphysical energy density resulting from the border region is minimizable. Even in that case our model does not have to be in line with the Friedmannian model, due to the additional effects of mass clumping.

5.3 Extreme input values

Now that we have come to some pretty interesting results, let us now discuss a potential flaw of our model and then try to derive how much sense the results would still make as a consequence. As already mentioned, the choice of the sets of input values is somewhat unrealistic. For instance our chosen cosmological constant is about 50 orders of magnitude larger than its measured value. Moreover, we obtained mass densities inside the sphere in the order of 10^{24} kg m^{-3}, which is about six orders of magnitude denser than a neutron star. Consequently, our toy universe is far from uniformly distributed. This is of course exactly what we are testing, however, this test would be particularly interesting in a more realistic case. Hence we would like to determine whether our conclusion of the previous section still holds, if we would have chosen somewhat more natural values for M, R and Λ.

First, we will argue that the values we have obtained so far are still useful, despite them being unrealistic. As already mentioned, we choose these large numbers, because otherwise the numerical errors would be too large. But on top of that, the number of digits of a float is limited. Consequently, when using more realistic numbers, certain dependencies may not have been noticeable, or perhaps the resulting $\overline{\rho}$ could have seemed to be zero after all. Hence, it may have been a blessing that we have used such extreme values.

Yet we have to take into account that when not using these extreme cases, special situations may not occur anymore after all, causing us to be not allowed to draw certain conclusions from the previous section. For instance, the positive value of $\overline{\rho}_B$ may not be present anymore, causing us to to be unable to conclude that the mass density resulting from the border region can vanish. So, let us now show that we can still create a toy universe using more realistic values, that is not in line with the Friedmannian model and in which the unphysical $|\overline{\rho}_B|$ is minimizable.

The dependence on certain input values in the less extreme regime may become minimal, but it is certainly not nonexistent anymore. Hence for $\Lambda = 0$ the average mass density will not always be exactly equal to zero all of a sudden. Similarly for $\Lambda = 1/18\ \mathrm{m}^{-2}$, $\overline{\rho}$ will not be exactly equal to $-2.977 \cdot 10^{24}\ \mathrm{kg\ m}^{-3}$ and hence the same can be said for (almost) any Λ. Consequently, we can still conclude that our model is not (always) in line with the Friedmannian model in the more realistic regime of input values.

Again, we would like to see if $|\overline{\rho}_B|$ remains minimizable. The dependence of $\overline{M}_B$ on d will logically still exist in the natural regime. I.e. for $\Lambda = 0$, $\overline{M}_B$ approaches zero from below for increasing d, whereas $\overline{M}_I$ remains constant. Hence we can still say that $|\overline{\rho}_B|$ is minimizable for $\Lambda = 0$. Meanwhile $\overline{\rho}$ remains positive, contradicting the first Friedmann equation.

Having chosen a specific M for $\Lambda \neq 0$, let us show that we can still make sure that $\overline{M}_B$ completely vanishes. By looking at tables 1 and 2 in the case $GM/c^2 = 1/108$ m, one can see that increasing Λ either causes $\overline{M}_B$ to increase or decrease, depending on the value of d. If it would cause $\overline{M}_B$ to decrease below zero, then we can simply increase d again to satisfy $\overline{M}_B = 0$. If it would cause $\overline{M}_B$ to increase to above zero, we have to decrease d again. But mind that we cannot decrease d to values smaller than $2R + b$ of course. So in that case we should actually lower Λ instead to obtain $\overline{M}_B = 0$ again.

Still for $\Lambda \neq 0$ there is no reason why $\overline{M}_I$ will suddenly become zero in the mean time, causing $\overline{\rho}_B$ to minimizable w.r.t $\overline{\rho}_I$. That is because a positive Λ only causes $\overline{M}_I$ to be bigger than the value of $\overline{M}_I$ for $\Lambda = 0$. For negative values of Λ, $\overline{M}_I$ would be smaller, however, we observed that our universe is accelerating and hence Λ must be positive. Hence we expect $\overline{M}_I$ to neither become zero, nor negative. Consequently, do not expect $\overline{\rho} = -\rho_{vac}$ to hold in the case that $\overline{M}_B$ completely vanishes.

In conclusion, it is still possible to minimise the average mass density resulting from the border region in the natural regime of input values, however, since we required $d > 2R + b$, it is not possible for all sets of input values. Also $\overline{\rho}$ will not suddenly become $-\rho_{vac}$. So now we can conclude that even in the natural regime, we will be able to create a universe (using this model) in which the border region does not contribute to the average mass density of the universe, while still not obeying the Friedmannian model. This is interesting since our modelled universe is still homogeneous at large, but apparently the mass clumps, that cause inhomogeneity at small scales introduce extra energy contributions, which was not expected by the first Friedman equation.

However, one has to keep in mind that in this model many assumptions have been made in an attempt to create a physical model, but yet unphysical negative mass densities existed in our toy universe. So we cannot conclude that the real universe is indeed not in line with the Friedmannian model due to mass clumping. Those extra mass densities may simply be an artefact of our toy model. But at least it indicates that the solution of the discrepancy between the two values of the Hubble parameter may very well be due to a lack of mass clumps in the Friedmannian model.

6 Outlook

For future research, it would at first be interesting to see whether the conclusions that have been drawn are indeed true, in the case that less extreme input values are used. In this research we have reached those conclusions using only a few sets of input values. However, we have not been able to actually see that they are indeed true. In order to obtain these numerical confirmations, one would need to adjust the computer program, such that it allows small values in the total metric without causing the resulting energy densities to be inaccurate, due to numerical precision limitations.

In future research, one could also make an adjustment to the definition of $S(x)$. In that case, other results could arise, which could result in different interesting conclusions. Yet there is no physical reason why one would have to prefer another definition of $S(x)$ satisfying the same requirements. It should simply cause the universe to be homogeneous on large scales and hence all cubes should look exactly the same. Apart from *smooth step functions*, which are similar to the one we used so far, one could also choose another *sigmoid function*, from which the smooth step functions are a family member. However, many sigmoid functions will ask more computation time than the one used in this thesis.

More importantly, it would be interesting to investigate what the effects of mass clumping is on the Hubble parameter directly. However, our model would not be very suitable for such research, because we demanded our universe to be static. Hence there was no possibility to see whether and how the masses could influence the evolution of our modelled universe. Consequently, we were unable to try to comprehend the discrepancy between the two different Hubble parameters. Hopefully, such a time dependent model, in which inhomogeneity on small scales due to mass clumping is taken into account, will cause the discrepancy between the two Hubble parameters to disappear.

All in all, we have been able to model a universe that does not obey the Friedmannian model due to the mass clumps causing inhomogeneity on small scales, even though homogeneity on large scales is still satisfied. Furthermore, in such a universe the effect of mass clumping is more significant if the modelled universe is less homogeneous at small scales. Fortunately, the unphysical negative mass densities turned out to be minimizable, though only artificially, even when using more natural sets of input values. The latter two statements make our model more consistent and physical and hence more reliable. Nonetheless, this model is in its current form unable

to compensate for the discrepancy between the two values of the Hubble parameter. Hence further research is needed, for instance to investigate how mass clumping can create extra compensating terms in the EFE, just like the terms introduced by Heinesen and Buchert [4]. In conclusion, this model hints that this discrepancy may very well be due to a lack of mass clumps in the Friedmannian model.

Acknowledgements

Last but not least, many thanks to D. Venhoek and W. Beenakker for their contributions and supervision during this bachelor project, and for their feedback on earlier versions of this thesis.

Appendices

A The real meaning of our quantities

Just for clarity, this section will elaborate on the real meaning of the quantities in our system. At the very start, we chose a coordinate transformation to simplify the general spherically symmetric metric from equation 3, making us able to derive the metric inside the sphere. The same trick has been applied in the derivation of the Schwarzschild metric. Hence from then on, all coordinates in this thesis are not the coordinates as one would expect them to be from our physical world.

In the derivation of the metric of a uniform sphere, we have defined a certain total mass M. But in these new coordinates this quantity does not really have a meaning other than that it can be called mass-like. The same holds for the density, which is constant in the new coordinate system, but not necessarily in the old one. When trying to derive the real mass, one would have to integrate using the determinant of the spatial components of the metric, as has been done for the density. This integration accounts for the curvature, which causes volumes to appear bigger as compared to flat spaces. After this integration the obtained values for the mass and densities are the correct ones and hence we do not anymore have to worry about the strange coordinates.

Even when we would have used the original coordinates, we would have to perform the integration, such that curvature is taken into account. In the end, it does not matter which coordinate system you use for this integration as for instance the resulting mass is independent of the chosen coordinate system. It is a property of the theory of General Relativity that any property is independent of the chosen coordinate system. If it would be dependent, the theory would fail, and up to now, the theory has been shown to be very consistent with observations. Hence, even though reality may be strange and hard to grasp in this strange new coordinate system, one is allowed to use it to simplify expressions.

One thing should be noted however. We defined and stacked the cubes using the special coordinates. But when you would transform back to real coordinates, you would find out that the surfaces of the border regions do not appear flat anymore, even when you would observe them in a flat Minkowski space. But we could as well have defined those cubes in the original coordinates, causing the integration bounds in each region to be different. Hence in the end, it does make a difference in which

coordinate system you define the cubes. However, again we are not modelling the real universe. We can in fact create any arbitrary model, satisfying some coordinate independent restrictions, and test what its properties are.

B Computer program notes

In this section a few additional remarks will be mentioned that may be needed to clarify the code, which we were unable to do in the text and the code.

Eventually in the computer program, the smooth step function is defined slightly differently, such that it takes a simpler form in the first octant, in order to save computation time. The function was defined such that it decreases from 1 to 0 on the positive side of the chosen axis. That means that the new smooth step function $S'(x)$ is defined as $S'(x) = 1 - S(x - d)$, such that:

$$S'(x) = \begin{cases} 1 & \text{if } x \leq \frac{1}{2}(d-b) \\ -2X^3 + 3X^2 & \text{if } \frac{1}{2}(d-b) < x < \frac{1}{2}(d+b) \text{ , where } X = -\frac{1}{b}\left[x - \frac{1}{2}(b+d)\right] \\ 0 & \text{if } x \geq \frac{1}{2}(d+b) \end{cases} \tag{53}$$

References

[1] A.G. Riess. The expansion of the universe is faster than expected. *Nat Rev Phys*, 2:10–12, 2020.

[2] Planck Collaboration. Planck 2018 results - VI. cosmological parameters. *A&A*, 641(A6), 2020.

[3] Tommaso Treu Licia Verde and Adam G. Riess. Tensions between the early and late universe. *Nature Astronomy*, 3(10):891–895, 2019.

[4] Asta Heinsen and Thomas Buchert. Solving the curvature and hubble parameter inconsistencies through structure formation-induced curvature. *Cass. Quantum Grav*, 37(164001), 2020.

[5] S. Carroll. *Spacetime and Geometry: Pearson New International Edition: An Introduction to General Relativity*. Pearson Education, 2014.

[6] G. W. Gibbons and S. W. Hawking. Cosmological event horizons, thermodynamics, and particle creation. *Phys. Rev. D*, 15:2738–2751, May 1977.

[7] A. Friedmann. Über die krümmung des raumes. *Z. Phys.*, 10(1):377–386, 1922.